音響性リポソームと超音波を使用した遺伝子薬物デリバリー

東北大学大学院医工学研究科医工学専攻
治療医工学講座分子デリバリーシステム研究分野
Yoko Yagishita 柳下陽子
Tetsuya Kodama 小玉哲也

近年開発された音響性リポソームは，気相と液相を同時に封入することが可能になり，遺伝子や薬物のキャリアとして使用されるだけでなく，超音波造影剤としても利用されるようになった．超音波の照射により音響性リポソームは容易に破壊され衝撃圧が発生する．この衝撃圧の作用で，隣接する細胞の膜透過性が促進され，封入された遺伝子や薬物は標的部位に導入される．この物理的手法は非侵襲性に優れ，非免疫原性であり，代表的な非ウイルスベクターとして注目されている．一方，分子導入に伴う治療効果は音響性リポソームの循環特性や，移動軌跡から再構築される微小血管の構造変化から評価されるものと期待される．
本稿では，音響性リポソームと超音波を使用した遺伝子薬物デリバリーについて概説し，筆者らが取り組んできた実験結果を紹介する．

KEY WORDS
◇ドラックデリバリーシステム（DDS）
◇細網内皮系統（reticuloendothelial system；RES）
◇腫瘍
◇PEG（polyethylen glycol）
◇キャビテーション
◇EPR効果（enhanced permeability and retention effect）
◇バブル
◇衝撃波

リポソームと音響性リポソーム

リポソームとは1層ないし数層の脂質二重膜で構成され，液相が封入された閉鎖系球体の総称である[1]．均一な粒径に調整することが可能であり，細胞や細胞内小器官に特定物質を運搬することができる．水溶性・脂溶性・両親媒性など異なる溶質を脂質膜で内包することが可能であり，このためこれらの溶質は外部環境からの不活化の作用を受けにくくなる．リポソーム膜に生体由来の脂質成分や，脂質末端にポリエチレングリコール（polyethylene glycol；PEG）を修飾させることで，細網内皮系統（reticuloendothelial system；RES）による排除作用を軽減させ，血液中に長く滞留させることができる．PEGには抗体やリガンドの結合が可能であり，病的組織への集積性や標的性を高めることができる[1]．DNAのデリバリーでは，正電荷を持つ脂質を膜成分とするカチオン性リポソームが使われることが多い．静電相互作用により負電荷であるDNAの脂質膜への吸着性を促進させることで，DNAの吸着量は10倍程度増加することが知られている[2]．

音響性リポソームとは，ガスが封入されたリポソームのことであり，一種の超音波造影剤である．超音波の波長に比べて粒子の直径が十分に小さい場合，超音波造影剤の散乱面積は半径の6乗と周波数の4乗，および体積弾性率，密度の組み合せで求められる．例えば，粒子直径が250 nmで臨床用超音波の周波数である3.5 MHzを使用する場合には，散乱面積は7×10^{-5} μm^2として計算される．今，超音波を単純に80 MHzに高めると散乱面積は19 μm^2程度に造影されることになる．したがって，高周波超音波を使用することで，微小血管内を移動する音響性リポソームを追跡することができる．また，この移動軌跡から血管像を抽出することで，血管構造の変化に伴う病巣の進展や治療効果の評価判定が期待される．生体内で超音波造影機能を安定に保持するために，水への拡散係数が低い高分

表1．リポソームと音響性リポソーム

	リポソーム	音響性リポソーム
構成脂質	リン脂質，コレステロール，DOPEなど	リン脂質，コレステロール，DOPEなど
ガスの封入	なし	あり C_3F_8，C_4F_{10}，SF_6
造影性	なし	あり
封入物質	脂溶性・水溶性薬剤/遺伝子	脂溶性・水溶性薬剤/遺伝子
外来分子の導入機序	fusion/endocytosis	バブルの崩壊やキャビテーションで生じる衝撃圧による細胞膜透過性の向上
表面の修飾	抗体・リガンド・PEGなど	抗体・リガンド・PEGなど
安定性	よい	悪い

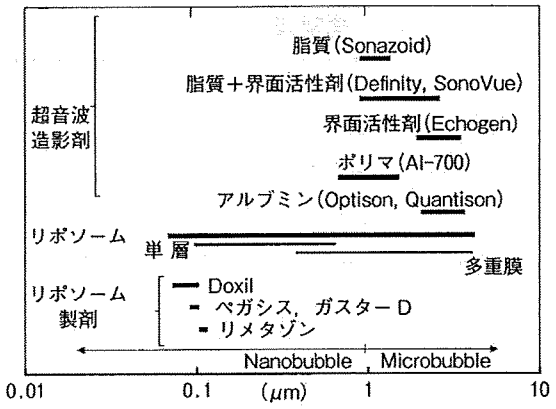

図1．様々な膜材料の超音波造影剤，およびリポソーム製剤の粒径分布

子ガス，例えば，パーフロロプロパン(C_3F_8)，パーフルオロブタン(C_4F_{10})あるいは六フッ化硫黄(SF_6)などがリポソーム内に封入される．表1にリポソームと音響性リポソームの特性を示しており，図1は，現在使用されている超音波造影剤およびリポソーム製剤の粒径分布である．超音波造影剤はその膜材料に関わらず数μmの範囲にあることがわかる．リポソームは多重膜リポソームと，単層リポソームに大別され，多重膜リポソームの直径が500～5,000 nmであるのに対し，単層リポソームは100～800 nmと小さい[3]．リポソーム製剤は60～120 nmの範囲に存在し，腫瘍新生血管からの高分子の流出・滞留効果，いわゆるEPR効果(enhanced permeability and retention Effect)に着目して開発された値になっている．例えば，ドキソルビシンのリポソーム製剤Doxilは直径70～100 nmである．

音響性リポソームの形態

音響性リポソームの内部構造は十分に理解されていないが，リポソームの作製方法の違いで，封入されるガスは脂質二重膜の層の間(図2A)[4]，あるいはリポソームの液相内に存在する一重膜構造のミセル内部(図2B)[5]，あるいは脂質一重膜のガス気泡内部(図2C)[6]に存在するものと考えられている．直径は，図2Aでは800 nm，図2Bは1～3μm，図2Cは100～200 nmであるといわれている[7]．図2Cに示すような，1つのマイクロバブル表面に何千ものリポソームを付加した小胞も開発されており，リポソームの付加に関わらずマイクロバブルとしての音響性は変化せずに薬剤の封入量の増加が確認されている．図2Dは筆者らが開発している音響性リポソームの透過型電子顕微鏡(TEM)観察結果の一部である[8]．膜成分はDSPE/DSPE-PEG2000である．液体(リン酸緩衝生理食塩水)とパーフロロプロパン(C_3F_8)が封入されていることが観察される．膜の厚さは約5.6 nmになっており，脂質二重膜の構造をとっているものと判断できる．しかし，このTEM結果のみでは，膜構造が図2Aなのか図2Bなのかを，判断することができない．

音響性リポソームと超音波を利用した遺伝子薬物デリバリー

リポソームによる外来分子の細胞内への導入は，一般的には拡散やエンドサイトーシスに起因して発生する．これに対し，音響性リポソームと超音波を併用し

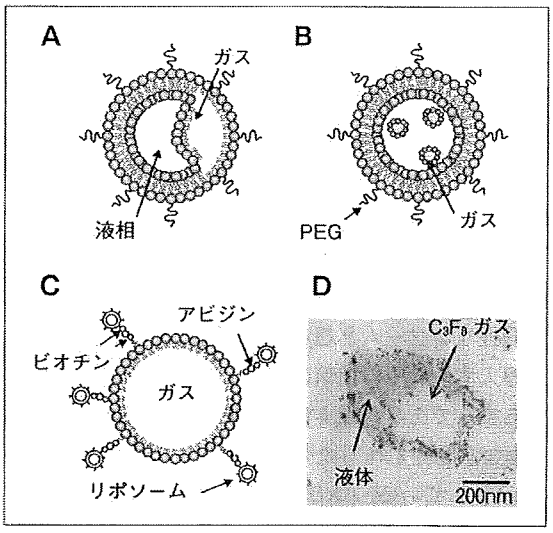

図2．音響性リポソームに封入されるガスの封入形態
ガスの封入形態には3つのモデルが提案されており，Aは脂質二重膜の層の間[4]，Bはリポソームの液相内に存在する一重膜構造のミセル内部[5]，Cは脂質一重膜のガス気泡表面にリポソームが付加されている[6]．直径は，Aでは800 nm，Bは直径1～3μm，Cでは100～200 nmであると報告される[7]．Dは筆者らが開発している音響性リポソームの透過型電子顕微鏡の観察画像である[16]．

た分子導入法は膜構造を物理的に変化させて外来分子を導入するものであり，エンドサイトーシスに依存しないものと考えられている．ガスが封入されているので，音響性リポソームは自由気泡と同じようにキャビテーション核として振舞う事ができる．超音波場にある音響性リポソームは超音波の照射圧を高める事で線形運動から非線形運動に振動モードが移行し，最終的には圧壊して衝撃圧を発生する．また音響性リポソームの破壊で放出されるガス，あるいは膜の破片に残留するガスからキャビテーション気泡が発生し衝撃圧が発生するものと考えられる．衝撃圧には気泡の振動や液体ジェット，衝撃波などが考えられており，超音波の照射条件や周囲の流動場の条件によって，これらの細胞への寄与度が異なる[9]．遺伝子薬物デリバリーの効率を高めるには，音響性リポソームを選択的に標的組織に集積させて，これらの衝撃圧を高める工夫が必要である．音響性リポソームの標的性を高める手法として，以下の3種類の方法が考えられる．

1．アクティブターゲティング

音響性リポソームの脂質膜に，標的組織に対する抗体や低分子のリガンドを結合させて，標的組織への選択的なデリバリーを実現する手法である．これは，特に副作用が問題となる抗癌剤への応用で注目されている手法である．

がん細胞が転移して増殖する際には血管が新生される．この新生血管の内皮には血管内皮細胞増殖因子受容体(VEGFR)-2をはじめ，多くの腫瘍マーカー(レセプター)が発現している．したがって，リポソームの脂質膜にこのマーカーに対するリガンドを組み込むことで(図3)，音響性リポソームは血流に沿って流れながら，レセプター・リガンド反応でこのレセプターに捕獲される．がん細胞を直接標的にする場合には，がん細胞の多くで過剰に発現しているトランスフェリン受容体(TFR)が標的にされることが多い．一般には，低分子のリガンドは，リポソーム表面の脂質膜に共有結合を介して結合させる．抗体など分子量の大きなリガンドを付加する場合には，アビジン・ビオチン結合を利用する．ただし，この方法は免疫原性がある

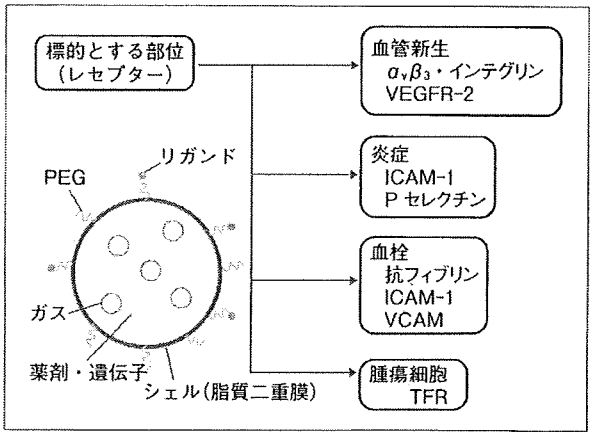

図3．アクティブターゲティング音響性リポソーム

と指摘されており，ヒトへの臨床応用が可能かどうかは不明である．

現在，筆者らは図3に示すような治療用分子(薬剤・遺伝子)を内包し，かつ膜表面には疾患部位を標的とするリガンドを組み入れた多くの治療性・標的性音響性リポソームを作製中であり，標的部位への治療分子の導入効率の改善を目指している．

2．パッシブターゲティング

パッシブターゲティングという概念は，腫瘍組織を標的としたリポソームの開発において重要である．ナノというサイズは，がん組織内に網羅された新しい血管ネットワーク(血管新生)から漏出するのに必要な粒子の直径として求められる値である．がん組織の新生血管は通常の血管と異なり，直径200 nm以下の粒子が血管壁から漏出・滞留する，いわゆるEPR効果が確認されている．この現象により，正常血管では血管外に漏出しにくい高分子物質も，腫瘍血管から漏出し，またその場に長く停滞するため，結果として高分子抗癌剤は選択的に癌組織に到達し，治療効果の向上と副作用の軽減が期待される．筆者らは音響性リポソームの粒径の制御から，EPR効果で，腫瘍組織内に音響性リポソームが集積する遺伝子薬物デリバリー法の開発を進めている．また，音響性リポソームの超音波画像からEPR効果を定量できるものと期待している．

3．二重超音波照射法

超音波の照射強度を制御する事で，標的部位に遺伝子や薬剤の効率的な導入を目指す二重超音波照射法が開発されている．

超音波場中に，音響性リポソームのような微細気泡が存在する場合，微細気泡は振動し，プライマリBjerknes力とセカンダリBjerknes力の二種類に区別される音響放射圧の作用を受ける．この現象に着目し，低い超音波で音響性リポソームを患部に移動させ，次に音圧の高い超音波を照射する事で音響性リポソームを破壊し，封入物質を患部に効率的に導入する手法が考えられる．これまで，低い音圧の超音波(50 kPa)，と高い音圧の超音波(2 MPa)を組み合わせた照射方法で，弱い超音波単独照射よりも10倍，強い超音波単独照射よりも0.5倍高く，細胞内にの蛍光色素の導入が達成されたとする報告がある[10]．

音響性リポソームによる分子導入

1．超音波照射条件

音響性リポソームと超音波を併用した分子導入法では，導入する分子の種類によって超音波の照射条件が異なるようである．図4はこれまで遺伝子と薬剤の導入実験で使用されてきた超音波の強さと周波数との関係が示されている．遺伝子の場合，超音波の強さは0.5～2.5 W/cm^2，周波数は1～3 MHzの範囲であるのに対して，薬剤の場合は強さも周波数もばらつきが大きい事がわかる．

2．キャビテーション気泡が介在する分子導入の機序

音響性リポソームが崩壊して球状のキャビテーション気泡が発生したと仮定しよう[9]．キャビテーション気泡の急激な半径方向の運動は壁面近傍の流体を圧縮・駆動する．この圧縮された液体には圧力波が形成される．圧力波の非線形波面は衝撃波面へと変形しな

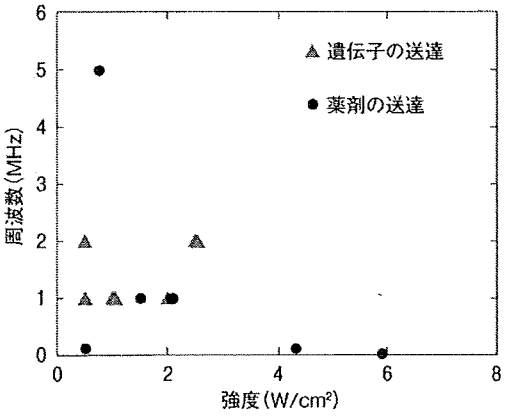

図4．遺伝子・薬剤デリバリーに関する超音波の周波数と強さとの関係

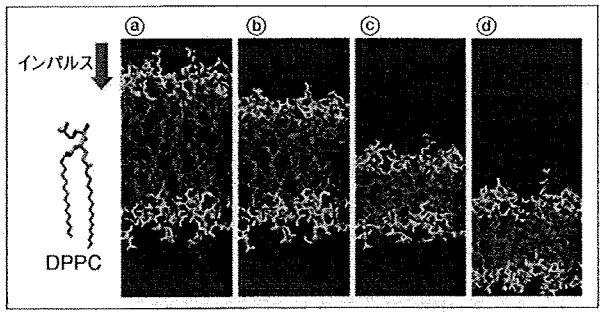

図5．衝撃波インパルス作用後の脂質二重膜の構造変化
衝撃波インパルスの作用を受けた脂質二重膜の変形を分子動力学シミュレーションで解析する．水分子を青色で表記し，アシル鎖は水分子の動きを理解しやすいように色付けをしていない．a：平衡状態，b：0.15 ps後には疎水基に水分子が移動しはじめる，c：0.30 ps，d：0.45 ps．平衡状態にあっても，水分子は疎水基に存在する．

がら，圧力波は衝撃波として伝播する．この衝撃波は気泡周囲の細胞と干渉して細胞膜の透過性を促し，外来分子の細胞内部への拡散に寄与するものと考えられる．衝撃波を分子動力学シミュレーションで記述すること自体，チャレンジングな課題であるが，いま衝撃波を衝撃波インパルス(衝撃波圧力の時間履歴を時間で積分した値)と定義して，細胞膜に衝撃波インパルスが作用したと仮定する．細胞膜は脂質とタンパク質からなる約5 nmの薄い二重膜である．ここでは脂質の主成分の1つであるジパルミトイルホスファチジルコリン(DPPC)で構成された脂質二重膜が水に浮かんだ状態に衝撃波インパルスが作用したと考える．**図5**は，衝撃波インパルスが上から下に向かって作用した場合のシミュレーションである．衝撃波インパルス作用後に脂質二重膜は大きく変形し，脂質外側にある水分子は脂質内に移動する[11]．水分子が強制的に脂質内に導入されると，やがて脂質膜に水孔が形成される事が示されており，外来分子はこの水孔から細胞内に導入されるのではと考えられる．

臨床への応用

1．局所投与が臨床に有効ながん

薬剤を導入する方法は，全身投与(静脈内注入，経口投与)と局所投与(動脈内注入，腹腔内投与，膀胱内投与等)に大別される．分子デリバリーの効率は全身投与より局所投与が1,000倍程度高いと指摘されている．局所投与と上記のEPR効果との相乗効果を考えると，本手法に適する「局所投与が臨床に有効ながん」は自ずと限定されてしまう．ここでいう「有効ながん」とは，本手法の有効性に期待でき，かつ既存の治療方法では治療効果に限度があり，新しい治療法の開発が望まれる「がん」として定義する．**表2**は，筆者らが考える「有効ながん」を示す．現在，筆者らは国立がんセンター東病院(松村保広 部

表2．局所投与が臨床に有効ながん

腫瘍	投与法	局所投与が有効である理由	死亡数(2005)	
			男性	女性
肝癌	動脈内投与 (肝動脈)	外科的手術後の再発率が高い(70 %)． 全身投与はほとんど効果がない． 手術と併用した局所投与が有効．	23,201	11,064
膀胱癌	膀胱内注入 動脈内投与 (内腸骨動脈・膀胱動脈)	外科的切除後の再発率が高い (50～70 %)、 手術と併用した局所投与が有効 (再発率30 %に抑制)．	4,141	1,888
卵巣癌	腹腔内投与	癌細胞が腹腔内に散在し，腹腔内で再発するリスクが高い．手術後に予防的に行なう．	—	4,467

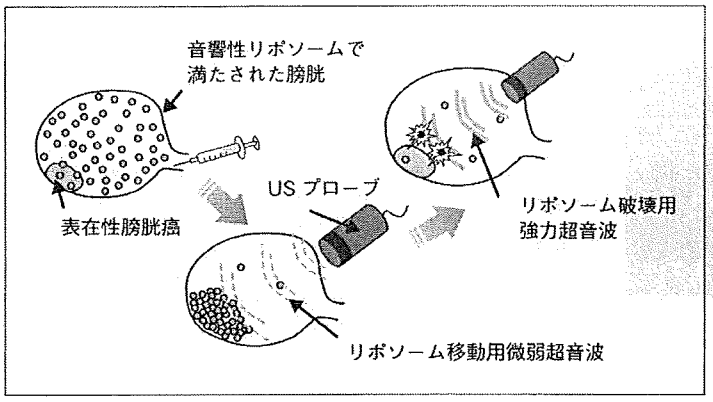

図 6．二重超音波照射法を利用した膀胱癌治療法の開発

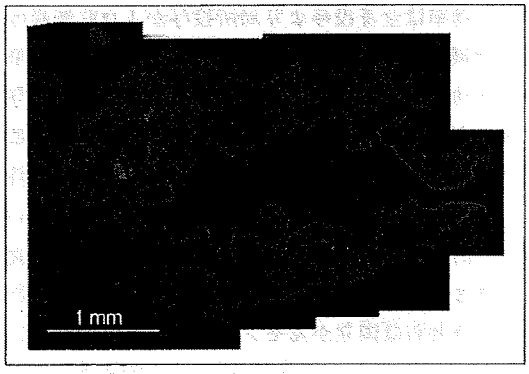

図 7．二重超音波照射法で膀胱内の目的部位に限局して導入された蛍光分子
赤：蛍光分子導入部位，青：膀胱横断面(DAPI 染色で細胞核を染色)

長)と臨床試験を念頭に，表在性膀胱癌を対象に共同研究を行なっている．膀胱癌は大きく分けて表在性膀胱癌，膀胱上皮内癌，浸潤性膀胱癌の 3 種類に分類されるが，ほとんどの場合は表在性膀胱癌であり，再発率は約 50～70％である．膀胱は閉鎖系であり，バブルの挙動の制御が容易である事から，前述の二重超音波照射法が有効である．最近，パーフロロプロパンが封入された音響性リポソームをマウスの膀胱内に注入し，二重超音波照射法でこのリポソームを目的部位に集積させて，膀胱壁に蛍光分子を導入させる事に成功した(図 6，7)．今後は，膀胱壁の全内壁にバブルを移動させて破壊させる事が可能な膀胱内挿入型超音波発生装置を開発し，臨床応用を目指す事を考えている．

2．血栓溶解

脳梗塞や心疾患で観察される血栓を超音波照射と音響性リポソームを併用し，溶解する手法が考案されている．この手法では超音波の照射で，音響性リポソームが成長・崩壊し，あるいはキャビテーション気泡が発生する事で血栓が砕かれるものと考えられる．血栓溶解剤(t-PA)を併用すると，超音波照射せず t-PA を単独で投与した場合と比較して 49.5％，血栓溶解効果の向上が確認されている[12]．血栓溶解剤放出特性は超音波照射で時間制御が可能である事から，この手法は臨床的意味づけが高いものと考えられている．

3．イメージングへの応用

図 3 で示したアクティブターゲティング型音響性リポソームと超音波を併用すると肝臓，脾臓，脳組織，冠動脈，腫瘍組織，炎症，感染症などで，超音波の画像診断の描出率や病的組織の解析率の向上が期待される．これまで，抗フィブリノーゲン抗体を組み込む事で血栓やプラークを標的としたリポソームや[13]，アテローム硬化症の診断を目的として，損傷血管内でのプラークの形成に関わる ICAM-1 や血管内皮細胞に発現する接着分子 VCAM に対する抗体を組み込んだリポソーム[13][14]，また腫瘍新生血管を標的とするために $\alpha_v\beta_3$ インテグリンを組み込んだリポソーム[16]等の開発が進められ，画像診断への応用が研究されている．これらの観察から，アクティブターゲティング型音響性リポソームを利用する事で，血管内にリポソーム注入後，約 5 分以内に疾患部位の超音波輝度値が増加する事や[15]，$\alpha_v\beta_3$ インテグリン標的に伴う造影感度が 27 倍増加する事が明らかになっている[16]．

現在の CT や MRI では直径 1 cm 以下の組織の塊

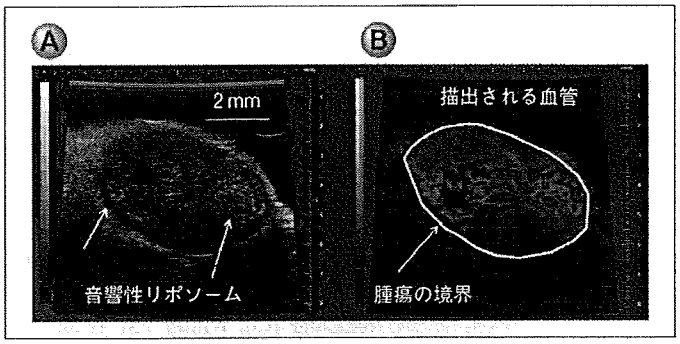

図8．A：マウスに移植された乳癌組織内の新生血管を流れるナノバブル(矢印)，B：バブルの移動軌跡から腫瘍新生血管が描写される．

が「がん」であると判断する事は難しい．現在，筆者らは音響性リポソームと80 MHzの高周波超音波を併用し，直径1 cm以下の腫瘍の早期診断法の開発に着手している．図8Aは，マウスに乳癌を移植し，癌組織内の血管を流れる音響性リポソームを中心周波数50 MHzの超音波で捉えた二次元画像である．図8Bはナノバブルの存在が確認される腫瘍血管像である．筆者らは平成20年10月から「マイクロバブルと超音波を用いた頭頸部癌症例の不顕性リンパ節転移検出の検討」と題して東北大学病院耳鼻咽喉・頭頸部外科で臨床試験を実施しており，血管の形状，密度，透過性を評価する事で血管新生の動的な解析だけでなく，抗腫瘍効果の評価も可能になるものと期待している．

おわりに

ドラッグデリバリーシステム(DDS)とは，体内動態を精緻に制御し，選択的かつ望ましい濃度－時間パターンのもとに薬物を作用部位に送達する事で，薬物治療の最適化を実現する事を目的にする新しい薬物の投与形態の総称として定義されている．しかし，最近の分子イメージングの進展を考慮すれば，薬物投与前の病的状態や薬物投与後の治療評価法を含めて，DDSを総合的な学問体系として広義に定義してはどうだろうか．この意味で，音響性リポソームと超音波を使用した遺伝子薬物デリバリー技術は治療・診断を即応できる新しいDDS手法として考えられるだろう．この技術の臨床応用の最大の課題は，細胞内への遺伝子薬物の導入効率の改善である．現在，筆者らは音響性リポソームを効率的に破壊するための超音波照射条件の最適化，長期に遺伝子の発現を誘導にするための長期発現プラスミドの開発，および臨床現場で応用可能なPETによる遺伝子発現のイメージング法の開発などを行なっており，近い将来，本技術の臨床応用を目指している．

◎文　献

1）Torchilin VP：Recent advances with liposomes as pharmaceutical carriers. *Nat Rev Drug Discov* **4**：145-160, 2005
2）Ferrara KW, Borden MA, Zhang H：Lipid-shelled vehicles：engineering for ultrasound molecular imaging and drug delivery. *Acc Chem Res* **42**：881-892, 2009
3）Samad A, Sultana Y, Aqil M：Liposomal drug delivery systems：an update review. *Curr Drug Deliv* **4**：297-305, 2007
4）Huang SL, MacDonald RC：Acoustically active liposomes for drug encapsulation and ultrasound-triggered release. *Biochim Biophys Acta* **1665**：134-141, 2004
5）Suzuki R, Takizawa T, Negishi Y, et al：Effective gene delivery with liposomal bubbles and ultrasound as novel non-viral system. *J Drug Target* **15**：531-537, 2007
6）Kheirolomoom A, Dayton PA, Lum AF, et al：Acoustically-active microbubbles conjugated to liposomes：characterization of a proposed drug delivery vehicle. *J Control Release* **118**：275-284, 2007
7）Huang SL：Liposomes in ultrasonic drug and gene

delivery. *Adv Drug Deliv Rev* **60** : 1167-1176, 2008
8) Kodama T, Tomita N, Horie S, et al : Morphological study on accoustic liposome using transmission electron microscopy. *J Electron Microsc.* 2009 (in press)
9) Kodama T, Tomita Y, Watanabe Y, et al : Cavitation bubbles mediated molecular delivery during sonoporation. *J BioSci BioEng* **4** : 124-140, 2009
10) Shortencarier MJ, Dayton PA, Bloch SH, et al : A method for radiation-force localized drug delivery using gas-filled lipospheres. *IEEE Trans Ultrason Ferroelectr Freq Control* **51** : 822-831, 2004
11) Koshiyama K, Kodama T, Yano T, Fujikawa S : Structural change in lipid bilayers and water penetration induced by shock waves : molecular dynamics simulations. *Biophys J* **91** : 2198-2205, 2006
12) Tiukinhoy-Laing SD, Buchanan K, Parikh D, et al : Fibrin targeting of tissue plasminogen activator-loaded echogenic liposomes. *J Drug Target* **15** : 109-114, 2007
13) Demos SM, Alkan-Onyuksel H, Kane BJ, et al : In vivo targeting of acoustically reflective liposomes for intravascular and transvascular ultrasonic enhancement. *J Am Coll Cardiol* **33** : 867-875, 1999
14) Klegerman ME, Hamilton AJ, Huang SL, et al : Quantitative immunoblot assay for assessment of liposomal antibody conjugation efficiency. *Anal Biochem* **300** : 46-52, 2002
15) Wickline SA, Neubauer AM, Winter PM, et al : Molecular imaging and therapy of atherosclerosis with targeted nanoparticles. *J Magn Reson Imaging* **25** : 667-680, 2007
16) Zhao S, Borden M, Bloch SH, et al : Radiation-force assisted targeting facilitates ultrasonic molecular imaging. *Mol Imaging* **3** : 135-148, 2004

Human Pathology (2009) 40, 542–551

ELSEVIER

Human
PATHOLOGY

www.elsevier.com/locate/humpath

Original contribution

Characterization of lymphangiogenesis in various stages of idiopathic diffuse alveolar damage

Masahiro Yamashita MD[a,*], Noriyuki Iwama MD[b], Fumiko Date[a], Ryoji Chiba MD[b], Masahito Ebina MD[c], Hiroshi Miki MD[d], Kohei Yamauchi MD[e], Takashi Sawai MD[f], Masato Nose MD[g], Shinobu Sato MD[h], Tohru Takahashi MD[i], Masao Ono MD[a]

[a]*Department of Pathology, Tohoku University Graduate School of Medicine, Sendai 980-8575, Japan*
[b]*Department of Pathology, Sendai Kosei Hospital, Sendai 980-8575, Miyagi, Japan*
[c]*Department of Respiratory and Molecular Medicine, Institute of Development, Aging, and Cancer, Tohoku University, Sendai 980-8575, Miyagi, Japan*
[d]*Department of Respiratory Medicine, Sendai Medical Center, Sendai 980-8575, Miyagi, Japan*
[e]*The Third Department of Internal Medicine, Iwate Medical University, Morioka, Iwate, Japan*
[f]*Department of Pathology, Iwate Medical University, Morioka, Iwate, Japan*
[g]*Department of Pathology, Ehime University School of Medicine, Toon, Ehime, Japan*
[h]*Department of Internal Medicine, Saka General Hospital, Shiogama, Miyagi, Japan*
[i]*Department of Pathology, Ishinomaki Red Cross Hospital, Ishinomaki, Miyagi, Japan*

Received 24 April 2008; revised 2 June 2008; accepted 2 June 2008

Keywords:
Pulmonary fibrosis;
Diffuse alveolar damage;
Lymphangiogenesis;
Capillary angiogenesis

Summary In pulmonary fibrosis, an abnormal healing process, is believed to be involved in the damage to lung tissue. This process has not been correlated with lymphangiogenesis, which has garnered current interest in relation to wound healing. The aim of the present study was to clarify the characteristics of lymphangiogenesis in pulmonary fibrosis associated with idiopathic diffuse alveolar damage. Formalin-fixed and paraffin-embedded lung tissues from 13 autopsy cases with idiopathic diffuse alveolar damage were used. Antibodies specific to CD34 and D2-40 were used to detect blood vessels and lymphatics, respectively, and immunohistochemical examinations and morphometry analyses were performed. The standardized density of capillaries was increased significantly in the exudative stage of diffuse alveolar damage, whereas that of the lymphatics remained unchanged. In the proliferative stage, new lymphatics emerged, primarily in the intra-alveolar fibrotic lesions where capillaries were absent. In the fibrotic stage, in which the lung was shrunken, as revealed by the elevated density of pulmonary arteries, the standardized density of capillaries was reduced significantly. The standardized area density of the interstitium was elevated in the proliferative stage and subsequently reduced in the fibrotic stage. Three-dimensional reconstruction of images revealed that some new lymphatics lacked connection to existing lymphatics. During the progression of diffuse alveolar damage, lymphangiogenesis occurs independent of capillary angiogenesis.

* Corresponding author.
E-mail address: yamam@mail.tains.tohoku.ac.jp (M. Yamashita).

0046-8177/$ – see front matter © 2009 Elsevier Inc. All rights reserved.
doi:10.1016/j.humpath.2008.06.031

1. Introduction

Diffuse alveolar damage (DAD) is a histologic manifestation of acute lung injury and is associated clinically with acute respiratory distress syndrome [1-4]. The condition also is manifested as an idiopathic disease, acute interstitial pneumonia [5-9]. These conditions generally are refractory to anti-inflammatory treatment and often cause lethal respiratory failure [1,5-9]. On the basis of histopathologic evidence, DAD is divided into 3 consecutive stages: exudative, defined by the formation of a hyaline membrane and edema of the alveolar wall; proliferative, defined by the presence of intra-alveolar fibrosis; and fibrotic, defined by the shrunken interstitium neighboring dilated air spaces (honeycomb formation) [1,4]. The mechanism by which DAD occasionally progresses to irreversible fibrosis of the lung is unclear.

Inflammatory fibrosis has been hypothesized as the explanation for the tissue destruction and fibrogenic remodeling associated with pulmonary fibrosis [10]. However, findings from experimental pulmonary fibrosis do not necessarily agree with this hypothesis. Mice deficient in the β6-integrin chain ($\beta6^{-/-}$) develop exaggerated inflammation. However, they are protected from bleomycin-induced pulmonary fibrosis, although a similar concentration of transforming growth factor-β was detectable in both $\beta6^{-/-}$ and $\beta6^{+/+}$ mice [11]. A fibrogenic response in the lung has been demonstrated in a mouse model of hyperoxic stress under blood-free conditions where the development of inflammation is limited [12]. Clinical outcomes in patients poorly compliant with anti-inflammatory therapy for DAD indicate that a pathogenic mechanism other than inflammatory fibrosis causes progression of the disease [10].

The lymphatic system plays various roles in fluid homeostasis and the activation of adaptive immunity by fluid drainage and cell transport [13]. Exploiting the ability to detect lymphatics by immunohistochemistry techniques, lymphangiogenesis has been discovered in various pathophysiological conditions [14-18], and its significance in tumor metastasis and wound healing has been postulated [19-23]. It has been demonstrated that in wound healing, lymphangiogenesis occurs after angiogenesis by the sprouting of existing lymphatics, and the resultant lymphatic system exists as a transient structure [22]. Lymphatics were observed to be less developed in a prolonged healing condition such as chronic skin ulcers than in normal healing [22]. It is reasonable to hypothesize that newly formed lymphatics play important roles in the later processes of wound healing, such as fibrosis.

Pulmonary fibrosis is believed to be a pathological consequence of wound healing in the lung [10]. We have focused on lymphangiogenesis in pulmonary fibrosis. The principal aim of this study was to characterize lymphangiogenesis in a fibrogenic condition associated with idiopathic DAD.

2. Materials and methods

2.1. Materials

We examined autopsy lung specimens of 11 men and 2 women with idiopathic DAD that were obtained from the archives of the Department of Pathology at Saka General Hospital, Ishinomaki Red Cross Hospital, Sendai Medical Center, or Iwate Medical University. Patients with idiopathic DAD fulfilled the clinical and pathological criteria for acute interstitial pneumonia described by Katzenstein et al [5]. None had any evidence of systemic infection, iatrogenic causes of immunosuppression, toxic exposure, cancer for which they were undergoing cytotoxic chemotherapy, or cardiac failure. Every patient had previously been healthy without established interstitial lung disease. All patients were observed to have acute onset of symptoms, severe hypoxemia, and diffuse pulmonary infiltrates on chest radiography and computed tomography scan. The mean age of the patients was 69.2 ± 5.5 years (range, 61-78 years). Every specimen was categorized into 1 of 3 consecutive stages of

Table 1 Primary antibodies used

Primary antibody	Source	Isotype	Antigen retrieval method	Concentration
CD34, NU-4A1 (Nichirei, Tokyo, Japan)	Mouse	IgG1	None	4
D2-40 (Dako Japan, Tokyo, Japan)	Mouse	IgG1	MW	0.26
Podoplanin (Angiobio, Del Mar, CA)	Mouse	IgG1	None	0.3
Cytokeratin, AE1/AE3 (Dako Japan)	Rabbit	IgG1 kappa	None	0.53
Prox-1 (Angiobio)	Rabbit	Polyclonal	MW	2
von Willebrand factor (Dako Japan)	Rabbit	Polyclonal	None	2.9
Laminin (Dako Japan)	Rabbit	Polyclonal	Trypsin+ pepsin	2
Vascular endothelial growth factor receptor-3 (R&D Systems, Minneapolis, MN)	Goat	Polyclonal	MW	0.4

NOTE. Trypsin and pepsin were applied for 30 minutes. Abbreviation: MW, microwave irradiation for 10 minutes in citrate buffer, pH 6.0.

DAD on the basis of morphologic criteria previously summarized by Travis et al [1]. Two stages were present in 4 cases. Normal lung tissues were obtained from 4 autopsies of patients who died independently of pulmonary diseases. All lungs were inflated by injecting 10% buffered formalin and embedded in paraffin wax.

The use of all autopsy samples was approved by The Ethical Committees of Saka General Hospital and Iwate

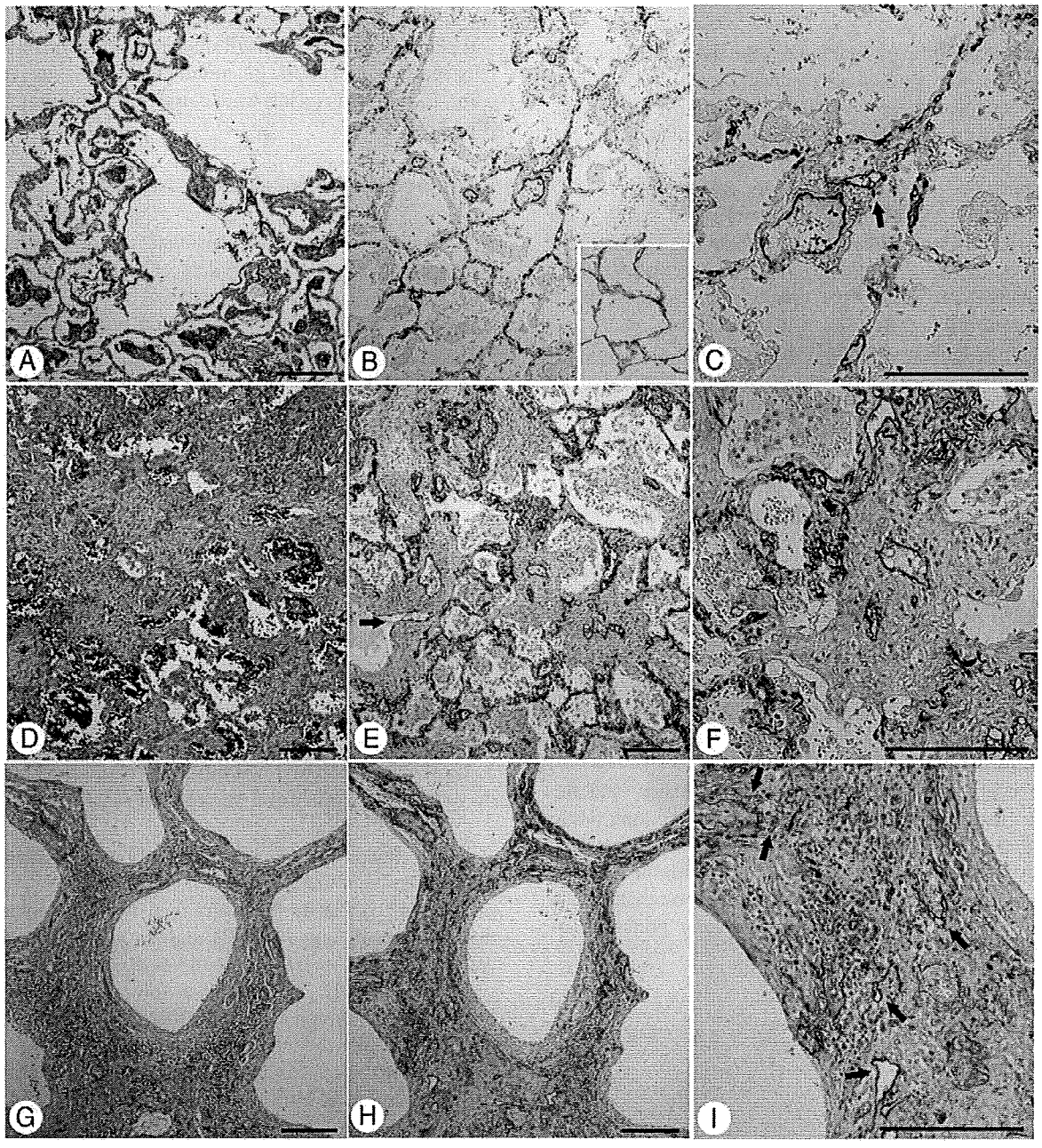

Fig. 1 Histopathologic and immunohistochemical characteristics of the 3 stages of DAD. A, Exudative stage represents mild fibrosis in alveolar wall and hyaline membrane in alveolar ducts. B and C, Number of $CD34^+$ capillaries (red) in alveolar wall is more than that in normal lung (inset in panel B). Existing lymphatics are shown as $D2\text{-}40^+$ (brown) around vessels (arrow). D, Proliferative stage represents increased fibrous thickening of alveolar wall and the presence of intra-alveolar fibrotic lesions. E and F, $D2\text{-}40^+$ lymphatics (brown) but not $CD34^+$ capillaries (red) are apparent in intra-alveolar fibrotic lesions. Heterotopic expression of D2-40 on surface of the intra-alveolar fibrotic lesion (arrow). G, Fibrotic stage exhibits dense interstitium, including collapsed alveoli and enlarged airspaces. H and I, Capillaries (red) and lymphatics (brown, arrows) in dense interstitium. A, D, and G, Elastica-Goldner stain; B, C, E, F, and I, dual immunostaining with CD34 and D2-40 counterstained by resorcin-fuchsin and hematoxylin. Scale bar, 200 μm.

Medical University and by the Institutional Review Board of Ishinomaki Red Cross Hospital and Sendai Medical Center. Informed consent was obtained from the bereaved family of every patient.

2.2. Immunohistochemical examination

We used the primary antibodies summarized in Table 1. Particularly, the antibodies against D2-40, podoplanin, vascular endothelial growth factor receptor-3 (VEGFR-3), and Prox-1 were used for the detection of lymphatics. For the negative controls for each antibody, mouse isotype-matched monoclonal IgG1 or mouse nonspecific IgG fraction (DAKO Japan), normal goat serum, and normal rabbit serum were used. After blocking with normal serum and incubation with antibodies, the antigen-antibody reaction was visualized by 3,3′-diaminobenzidine tetrahydrochloride. Sections were counterstained by resorcin-fuchsin and hematoxylin.

Dual immunohistochemical staining using CD34 and D2-40, von Willebrand factor, and D2-40 was performed as described previously [24]. Antigen-Antibody reactions were visualized by Vector Red (Vector Laboratories, Burlingame, CA) and 3,3′-diaminobenzidine.

2.3. Morphometry of vascular densities and interstitial area

The numerical density of pulmonary arteries (N_A(PA)) and CD34-positive capillaries (N_A(cap)), the length density of D2-40–positive lymphatic endothelium (L_A(ly)), and the area density of interstitium (A_A(int)) were estimated on overlapping serial sections by a square centimeter grid [25]. Morphometric examinations were performed independently by the 2 pathologists (M.Y. and M.O.).

The degrees to which capillaries, lymphatics, and the volume change of interstitium developed in the lung tissue were quantified in terms of their length density in space (L_V(cap)), the surface density (S_V(ly)), and the volume density (V_v(int)), respectively. These were estimated in a unit area of lung section resorting to basic principles of stereology [25]:

$$L_V(\text{cap}) = 2N_A(\text{cap}) \quad (1)$$

$$S_V(\text{ly}) = 4L_A(\text{ly})/\pi \quad (2)$$

$$V_v(\text{int}) = A_A(\text{int}) \quad (3)$$

Here, N_A(cap), L_A(ly), and A_A(int) are, respectively, the numerical densities of the capillaries, the length density of the lymphatic walls, and the fraction of interstitium, all in terms of area. N_A(cap) was estimated by counting $CD34^+$ capillary number in a grid section of an ocular. L_A(ly) was estimated by measuring the perimeter lengths of the linear profiles of $D2\text{-}40^+$ lymphatics using a projector (V-16C, Nikon, Tokyo, Japan) and a digitizer (Motic Images Plus 2.0S image analysis system).

The shrinkage of existing structures associated with disease progression produces stage-specific deviation. To compare stage-specific data under such deviated conditions, the numerical density, N_A(PA), of muscular pulmonary arteries with an external diameter larger than 100 μm was calculated on the basis of microscopic observations on lung sections, and all the quantitative results denoted as N_A(cap), L_A(ly), and A_A(int) were corrected by dividing by N_A(PA) [26].

2.4. Three-dimensional reconstruction

Reconstruction of 3-dimensional (3-D) images was achieved from 2-dimensional data of serial tissue sections [27]. Briefly, images of lymphatics as D2-40–positive structures were magnified and copied onto tracing paper using a profile projector (V-16C, Nikon). The images on the tracing papers were extracted using a digitizer system (Wacom, Saitama, Japan), and the 3-D image was reconstructed (OZ95; Rose, Sendai, Japan).

2.5. Statistical analysis

The statistical significance of differences between any 2 pairs of the 3 groups was evaluated using Tukey test. A P value less than .05 was considered significant.

3. Results

3.1. Stage-specific histopathologic characteristics of lymphatic and blood vessels in DAD progression

In the exudative stage, characterized by the formation of the hyaline membrane and mild fibrosis (Fig. 1A), greater numbers of capillaries were observed in the alveolar wall than in normal lung (Fig. 1B and C, inset). Lymphatics were observed around large blood vessels and in the lobular septa, as generally observed in a normal lung (Fig. 1C). Hereafter, the lymphatics with these characteristics are termed "existing lymphatics." In the proliferative stage, characterized by the fibrous thickening of the alveolar wall and the presence of intra-alveolar fibrotic lesions (Fig. 1D), lymphatics of various sizes frequently were observed in the lesions, whereas capillaries were undetectable (Figs. 1E and F). Because these lymphatics were observed to emerge in a disease-associated manner, they are termed "newly formed lymphatics" in this article. Heterotopic expression of D2-40 was observed on the surface of the intra-alveolar fibrotic lesions, particularly in the early proliferative stage, although this expression was limited in the later proliferative stage. In the fibrotic stage, characterized by

temporally homogenous remodeling structures that consisted of dense interstitium and enlarged airspaces (Fig. 1G), collapsed capillaries and lymphatics were observed in the interstitium (Fig. 1H, F). The intensity of collagen staining was increased compared with the proliferative stage (Fig. 1G).

Using serial sections, we confirmed the coexpression of other lymphatic markers, namely, podoplanin, VEGFR-3, and Prox-1, on D2-40$^+$ endothelial cells of the newly formed and existing lymphatics (Fig. 2A-F). Other blood vessel markers, such as von Willebrand factor and laminin, were not detected on the D2-40$^+$ cells, indicating that the D2-40$^+$

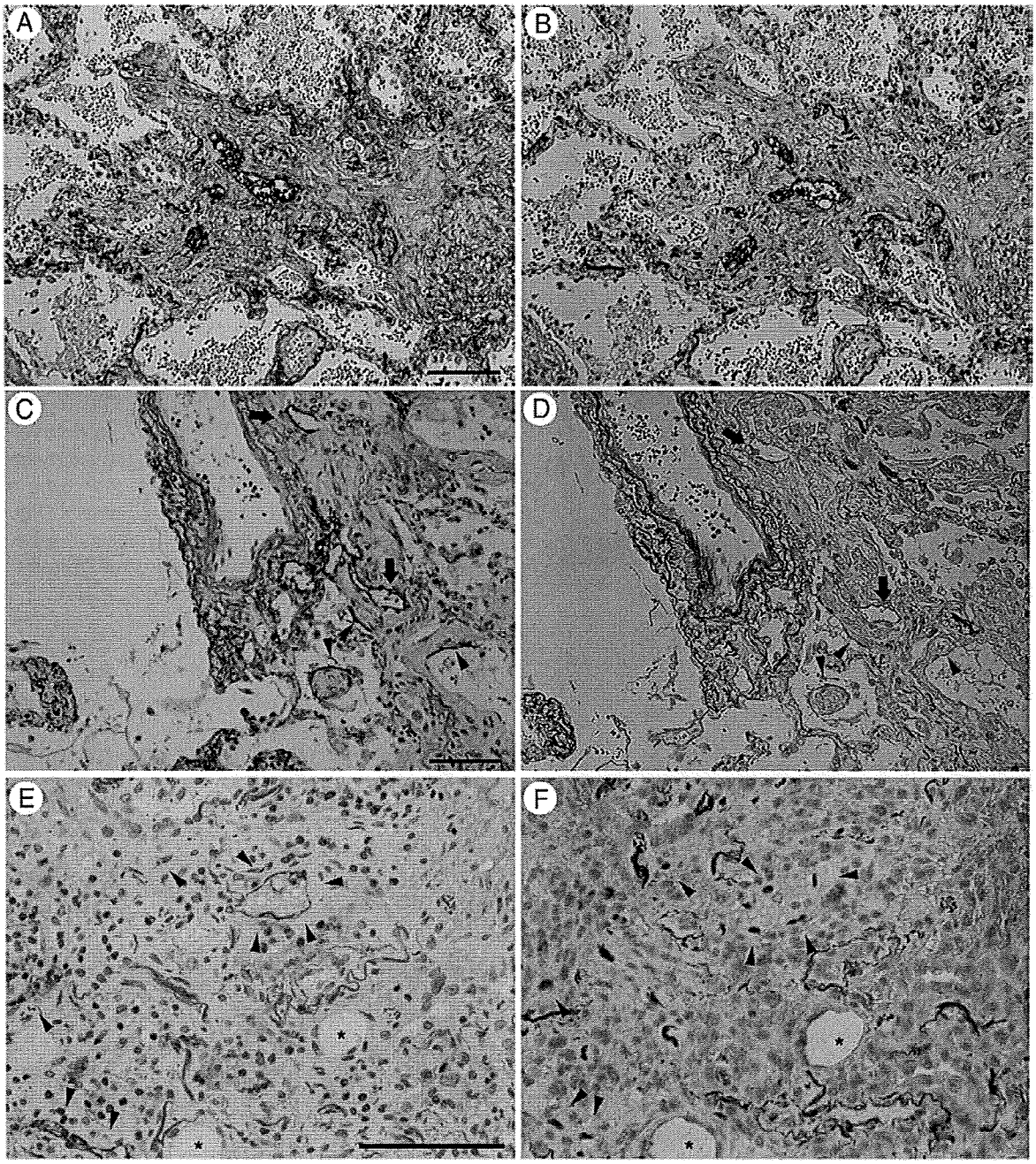

Fig. 2 Colocalization of podoplanin, VEGFR-3, and Prox-1 with D2-40. A and B, Immunostaining of serial sections shows colocalization of (A) D2-40 and (B) podoplanin in both existing and newly formed lymphatic vessels. C and D, Immunostaining of serial sections shows colocalization of (C) D2-40 and (D) VEGFR-3 in both existing and newly formed (arrows) lymphatics. Heterologous colocalization of D2-40 and VEGFR-3 on surface of intra-alveolar fibrotic lesion (arrowheads). E and F, Immunostaining of serial sections shows colocalization of D2-40 (E) and Prox-1 (F) in newly formed lymphatics (arrowheads). Resorcin-fuchsin and hematoxylin for counterstaining. Scale bar, 100 μm.

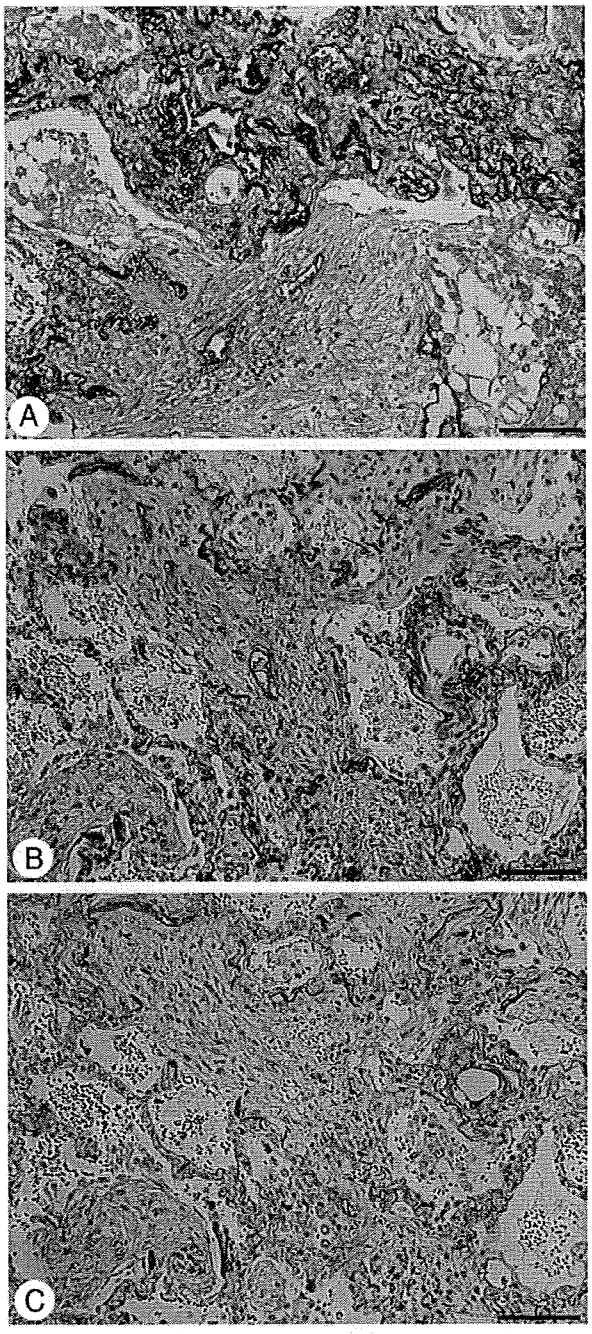

Fig. 3 Dissociated expression of von Willebrand factor (vWF) and laminin from D2-40 expression in intra-alveolar fibrotic lesions. A, Dual immunostaining for vWF and D2-40 counterstained by resorcin-fuchsin and hematoxylin shows that vWF is absent in the intra-alveolar fibrotic lesion, in which D2-40 is expressed. B and C, Immunostaining of serial sections shows that laminin-positive vessels are absent in intra-alveolar fibrotic lesions, where D2-40 is expressed (B), whereas laminin is expressed in a blood vessel (C). Scale bar, 100 μm.

vessels differed from the blood vessels with regard to identifying characteristics (Fig. 3A-C). Neither marker was expressed in the intra-alveolar fibrotic lesions.

3.2. Morphometry analyses

Pulmonary artery density (N_A(PA)), standardized capillary density (N_A(cap)/N_A(PA)), standardized lymphatic density (L_A(ly)/N_A(PA)), and standardized interstitial density (A_A(int)/N_A(PA)) were estimated in normal lungs (n = 4) and DAD in the exudative (n = 5), proliferative (n = 8), and fibrotic (n = 4) stages. The N_A(PA) values in the normal lungs and the 3 stages were 5.3 ± 1.7, 6.3 ± 2.4, 11.3 ± 3.03, and 17.6 ± 3.68/cm^2, respectively (Fig. 4A). The N_A(PA) values in the proliferative and fibrotic stage were significantly higher than that in the previous stage (P < .05). The N_A(cap)/N_A(PA) values in the normal lungs and the 3 stages were 1735.3 ± 484.40, 2679.5 ± 452.57, 3096.6 ± 399.57, and 988.2 ± 338.7, respectively (Fig. 4B). The density in the exudative stage was significantly higher than that in normal lungs (P < .05), whereas the density in the fibrotic stage was significantly lower than that in the proliferative stage (P < .001). These results indicate that the capillary network develops early in or before the exudative stage and regresses in the fibrotic stage. The L_A(ly)/N_A(PA) values of existing lymphatics in the normal lungs and the 3 stages were 5943.2 ± 1581.5, 5503.0 ± 2012.0, 5203.2 ± 1999.6, and 4378.1 ± 916.07, respectively, and the L_A(ly)/N_A(PA) values of newly formed lymphatics were 4068.2 ± 1821.4 and 3796.4 ± 996.45 in the proliferative and fibrotic stages, respectively (Fig. 4C). These findings indicate that the lymphatic network is newly formed exclusively in the proliferative stage, whereas existing lymphatics exist throughout the 3 stages. The A_A(int)/N_A(PA) values in the normal lungs and the 3 stages were 228.9 ± 33.00, 414.5 ± 106.4, 621.4 ± 88.00, and 221.2 ± 60.52, respectively (Fig. 4D). There were statistically significant differences between the normal lungs and the exudative stage, between the exudative and proliferative stages (P < .05), and between the proliferative and fibrotic stages (P < .001).

3.3. Characteristics of newly formed lymphatics in the proliferative stage

Immunohistochemical analyses using serial tissue sections with 3-D reconstruction demonstrated discontinuity between some newly formed and existing lymphatics in the proliferative stage, although some of the new lymphatics connected with existing ones (Fig. 5Aand B). In addition, D2-40 expression on the surface of the intra-alveolar fibrotic lesion continued to the lymphatic lumen (Fig. 5A and B), and further immunohistochemical analysis using serial sections revealed that the surface cells with heterologous D2-40 expression expressed VEGFR-3 but not the epithelial cell marker cytokeratin AE1/AE3 (Figs. 2C and D and 5C and D). In the later proliferative stage, no newly formed lymphatics were

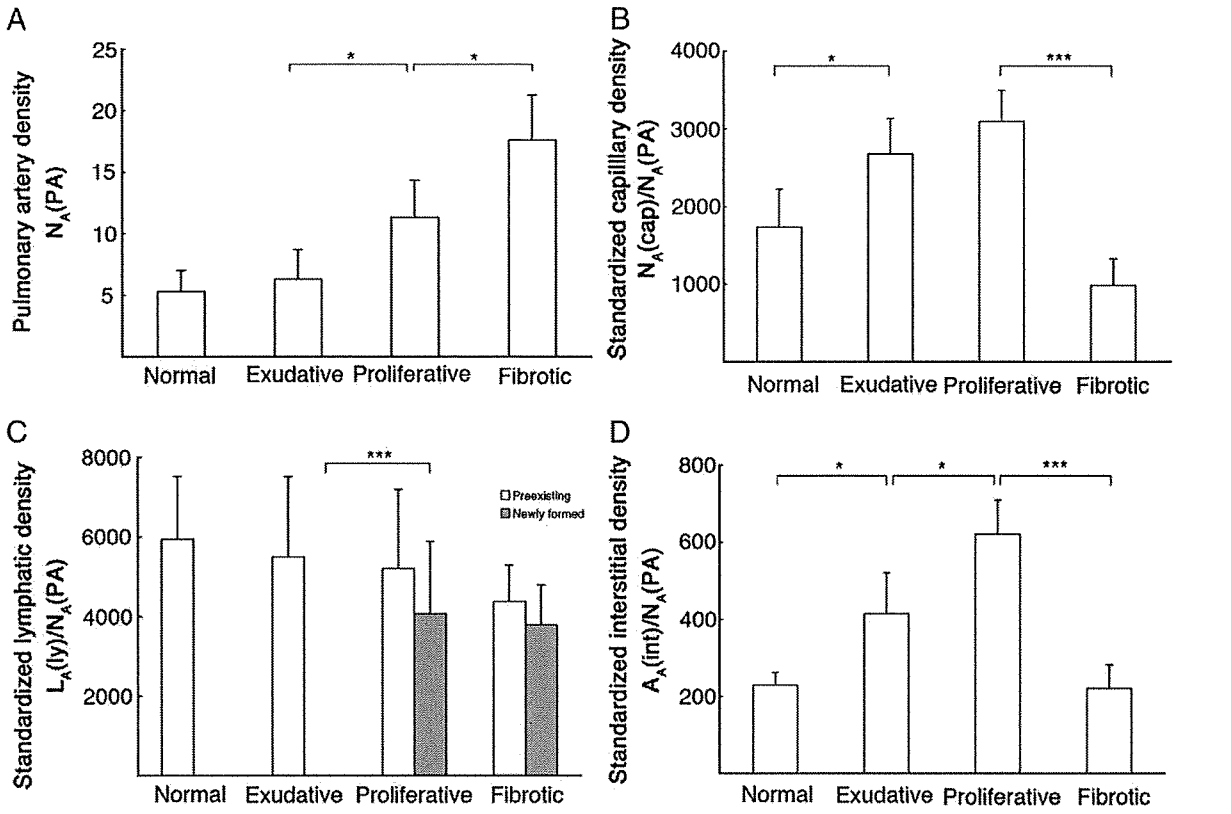

Fig. 4 Morphometry data from specimens in exudative (n = 5), proliferative (n = 8), and fibrotic (n = 4) stages of DAD. Data are shown as mean ± SD. A, Pulmonary artery density: N_A(PA). B, Standardized capillary density: N_A(cap)/N_A(PA). C, Standardized lymphatic density: L_A(ly)/N_A(PA). D, Standardized interstitial density: A_A(int)/N_A(PA). $^*P < .05$; $^{**}P < .01$; $^{***}P < .001$.

observed in the intra-alveolar fibrosis without connection to existing ones (Fig. 6A-C).

4. Discussion

The present study confirmed stage-specific characteristics during the progression of idiopathic DAD, particularly with regard to lymphangiogenesis and capillary angiogenesis. The results lead to new insights, revealing that robust lymphangiogenesis occurs in intra-alveolar fibrotic lesions in the proliferative stage of DAD. On the other hand, capillary angiogenesis was observed to occur early in the exudative stage and subsided thereafter. Notably, capillary angiogenesis was induced to a limited extent in the intra-alveolar fibrotic lesions. In the fibrotic stage, it was evident that blood vessels regress while lymphatics persist. There is limited information regarding the role of the lymphatic system in pathological fibrosis. Our present findings shed new light on this role and will facilitate further investigations into the differential roles of lymphangiogenesis and capillary angiogenesis in pulmonary fibrosis.

The temporal and anatomic correlation of lymphangiogenesis and capillary angiogenesis has been demonstrated in animal models of cutaneous wound healing and bronchitis with *Mycoplasma pulmonis* infection [22,28]. Under these conditions, capillary angiogenesis preceded lymphangiogenesis, and new lymphatics sprouted from existing ones. Proliferation eventually resulted in an intertwined structure of blood and lymphatic vessels; however, this structure regressed in the late stage of wound healing. These findings suggest the significance of the temporal and anatomic correlation of lymphangiogenesis and capillary angiogenesis and the regression of this structure for the completion of wound healing. In the case of DAD, although lymphangiogenesis follows capillary angiogenesis, new lymphatics are formed mainly in the intra-alveolar fibrotic lesions, where blood vessels are absent, and these newly formed lymphatics are anatomically separated from the capillary network. It also is characteristic that lymphatics persist in the fibrotic stage. Matsui et al [29] reported a relatively high density of lymphatics in an experimental renal fibrosis model in rats; the density of the blood vessels was significantly decreased in this area compared with that in a normal interstitial region. In a normal kidney, the presence of lymphatics is restricted to the regions around the interlobular arteries. A lymphatic-dominant lesion in the kidney may be established by lymphangiogenesis in the absence of both preceding capillary angiogenesis and eventual lymphatic regression,

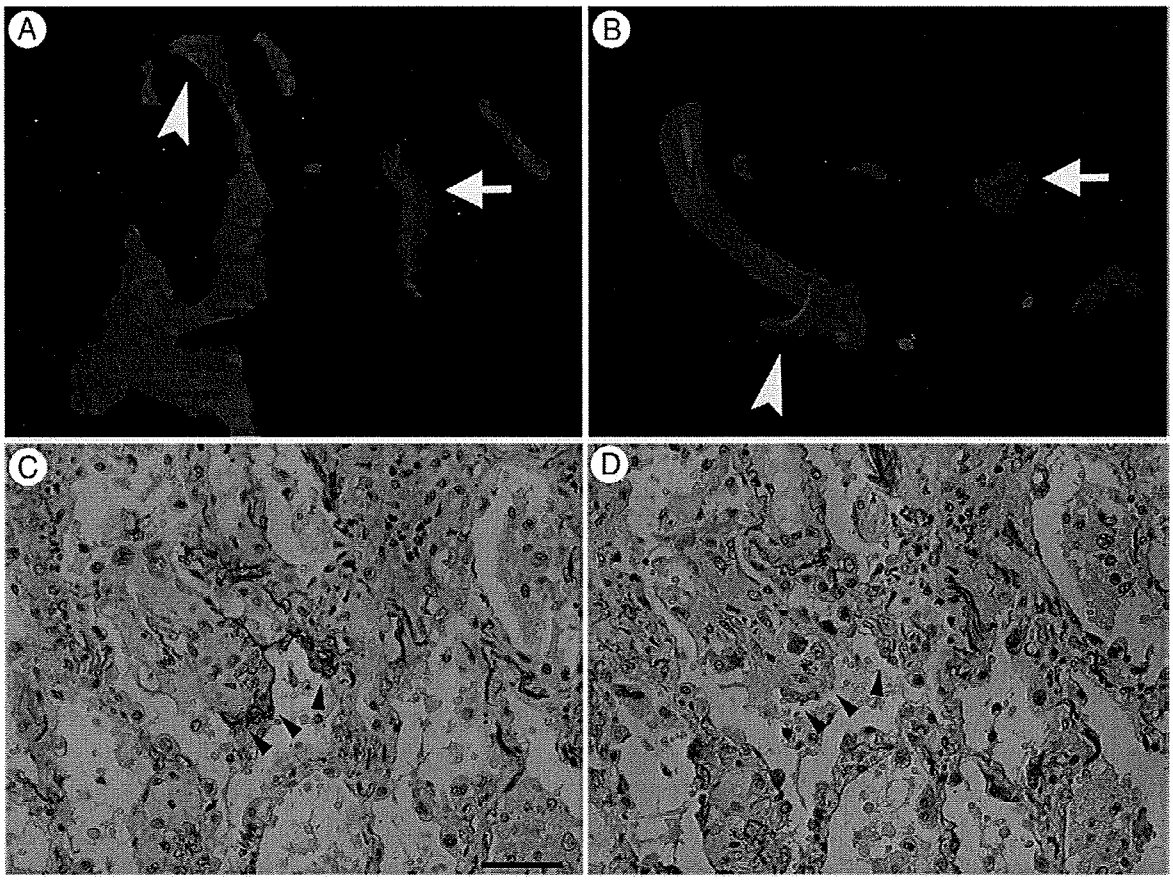

Fig. 5 Characteristics of lymphatic structures in proliferative stage of DAD. Overhead (A) and lateral (B) views of D2-40$^+$ structure revealed by 3-D reconstruction show isolated lymphatic structure from existing lymphatics (arrows) and continuation between surface expression of D2-40$^+$ on intra-alveolar fibrotic lesions and lymphatic vessel in this lesion (arrowheads). The 3-D images are reconstructions of 50 slices encompassing 200-μm thickness of lung tissue. C and D, Serial sections show that D2-40$^+$ cells (arrowheads in panel C) heterologously present on surface of intra-alveolar fibrotic lesions are not colocalized with cytokeratin-positive cells. Scale bar, 100 μm.

as in our cases. It is an important question whether the presence of lymphatic-dominant lesions is characteristic of irreparable fibrosis.

By morphometry analysis, the standardized interstitial density was decreased significantly in the fibrotic stage. The gross evaluation of the intensity of collagen staining revealed that collagen density in a representative lesion was increased remarkably compared with the proliferative stage. These observations imply that the lymphatics persisting in the fibrotic stage of DAD may contribute to the decrease in the standardized interstitial density via fluid drainage. This function may eventually facilitate the architectural remodeling associated with honeycomb lung. Further studies are needed to investigate whether this decrease is attributable to collagen absorption.

Keane et al [30] documented high levels of angiogenic cytokines in the bronchoalveolar lavage fluid obtained from patients with early acute respiratory distress syndrome. We demonstrated higher standardized capillary density in the alveolar wall in the exudative stage in our specimens. In low-grade fibrosis in idiopathic pulmonary fibrosis, CD34$^+$ capillaries were increased in the alveolar wall [31]. In fibrogenic pulmonary disorders, capillary angiogenesis may occur in the early phase, possibly contributing to the fibrogenesis. On the other hand, CD34$^+$ capillaries were barely detectable in the fibroblastic foci in idiopathic pulmonary fibrosis [31-33]. We demonstrated that the intra-alveolar fibrotic lesions of DAD included few CD34$^+$ capillaries. In contrast, Masson's body—an organized fibrotic lesion that manifests in cryptogenic organizing pneumonia—was observed to contain many capillaries [34]. Cryptogenic organizing pneumonia is reversible; moreover, fibrosis of Masson's body is repairable. Our findings of capillary angiogenesis in DAD are similar to those in idiopathic pulmonary fibrosis. It is interesting to debate whether the absence of capillary angiogenesis in intra-alveolar fibrotic lesions is associated with a poor prognosis in fibrogenic pulmonary disorders.

Unexpectedly, we demonstrated that D2-40$^+$ cells were frequently present on the surface of intra-alveolar fibrotic lesions in the proliferative stage. This heterotopic expression of D2-40 was observed to only a limited extent in the fibrotic

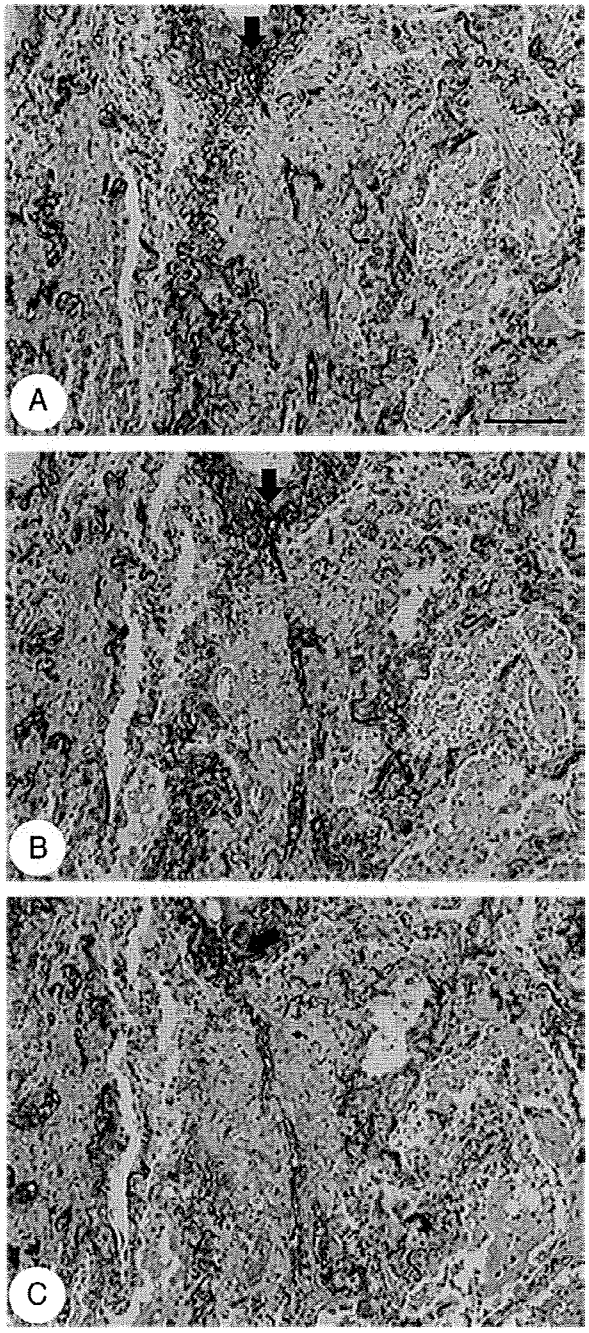

Fig. 6 Connection between newly formed and existing lymphatics in later proliferative stage. Serial sections show that collapsed D2-40$^+$ lumens in intra-alveolar fibrotic lesions connect to an existing one in the later proliferative stage, where alveoli tend to be collapsed. Arrows indicate existing lymphatic vessel around blood vessel. Scale bar, 100 μm.

stage. Analysis of serial tissue sections confirmed that these cells express VEGFR-3, an essential growth factor receptor for lymphatic endothelial cells, whereas these cells did not express the epithelial marker AE1/AE3, demonstrating the character of lymphatic endothelial cells. Furthermore, 3-D reconstructions of serial D2-40-stained sections clearly depicted continuity between these heterotopic and usual lymphatic structures in the intra-alveolar fibrotic lesions. The function of the open structure of lymphatics in DAD remains unknown. Some newly formed lymphatics in the intra-alveolar fibrotic lesions had no connection with the existing lymphatics, suggesting a unique mode of lymphangiogenesis in DAD that differs from the sprouting mode detectable as the conventional process in inflammation.

In conclusion, during the progression of idiopathic DAD, lymphangiogenesis occurs independent of capillary angiogenesis. Understanding the roles of capillary angiogenesis and lymphangiogenesis in pulmonary fibrosis may contribute to recognition of new treatment strategies for aberrant tissue repair.

Acknowledgments

We would like to thank Dr Keiichi Saito, Mrs Naoko Shibata, Mr Koichi Sato, and Dr Toshio Kumasaka for their excellent help.

References

[1] Travis WD, Colby TV, Koss MN, et al. Non-neoplastic disorders of the lower respiratory tract. In: West King D, editor. Atlas of non-tumor pathology. Washington, DC: American Registry of Pathology and Armed Forces Institute of Pathology; 2002. p. 89-106.

[2] Bachofen M, Weibel ER. Alterations of the gas exchange apparatus in adult respiratory insufficiency associated with septicemia. Am Rev Respir Dis 1977;116:589-615.

[3] Gould VE, Tosco R, Wheelis RF, et al. Oxygen pneumonitis in man: ultrastructural observations on the development of alveolar lesions. Lab Invest 1972;26:499-508.

[4] Katzenstein AL, Bloor CM, Leibow AA. Diffuse alveolar damage—the role of oxygen, shock, and related factors. A review. Am J Pathol 1976;85:209-28.

[5] Katzenstein AL, Myers JL, Mazur MT. Acute interstitial pneumonia: a clinicopathologic, ultrastructural, and cell kinetic study. Am J Surg Pathol 1986;10:256-67.

[6] Sugiyama K, Kawai T. Diffuse alveolar damage and acute interstitial pneumonitis: histochemical evaluation with lectins and monoclonal antibodies against surfactant apoprotein and collagen type IV. Mod Pathol 1993;6:242-8.

[7] Bouros D, Nicholson AC, Polychronopoulos V, et al. Acute interstitial pneumonia. Eur Respir J 2000;15:412-8.

[8] Bonaccorsi A, Cancellieri A, Chilosi M, et al. Acute interstitial pneumonia: report of a series. Eur Respir J 2003;21:187-91.

[9] Olson J, Colby TV, Elliott CG. Hamman-Rich syndrome revisited. Mayo Clin Proc 1990;65:1538-48.

[10] Selman M, King TE, Pardo A, American Thoracic Society, European Respiratory Society, American College of Chest Physicians. Idiopathic pulmonary fibrosis: prevailing and evolving hypotheses about its pathogenesis and implications for therapy. Ann Intern Med 2001;134:136-51.

[11] Munger JS, Huang X, Kawakatsu H, et al. The integrin alpha v beta 6 binds and activates latent TGF beta 1: a mechanism for regulating pulmonary inflammation and fibrosis. Cell 1999;96:319-28.

[12] Adamson IY, Young L, Bowden DH. Relationship of alveolar epithelial injury and repair to the induction of pulmonary fibrosis. Am J Pathol 1988;130:377-83.
[13] Ji RC. Characteristics of lymphatic endothelial cells in physiological and pathological conditions. Histol Histopathol 2005;20:155-75.
[14] Kaipainen A, Korhonen J, Mustonen T, et al. Expression of the fms-like tyrosine kinase 4 gene becomes restricted to lymphatic endothelium during development. Proc Natl Acad Sci USA 1995;92:3566-70.
[15] Banerji S, Ni J, Wang SX, et al. LYVE-1, a new homologue of the CD44 glycoprotein, is a lymph-specific receptor for hyaluronan. J Cell Biol 1999;144:789-801.
[16] Breiteneder-Geleff S, Soleiman A, Kowalski H, et al. Angiosarcomas express mixed endothelial phenotypes of blood and lymphatic capillaries: podoplanin as a specific marker for lymphatic endothelium. Am J Pathol 1999;154:385-94.
[17] Petrova TV, Makinen T, Makela TP, et al. Lymphatic endothelial reprogramming of vascular endothelial cells by the Prox-1 homeobox transcription factor. EMBO J 2002;21:4593-9.
[18] Kahn HJ, Bailey D, Marks A. Monoclonal antibody D2-40, a new marker of lymphatic endothelium, reacts with Kaposi's sarcoma and a subset of angiosarcomas. Mod Pathol 2002;15:434-40.
[19] Williams CS, Leek RD, Robson AM, et al. Absence of lymphangiogenesis and intratumoural lymph vessels in human metastatic breast cancer. J Pathol 2003;200:195-206.
[20] Skobe M, Hawighorst T, Jackson DG, et al. Induction of tumor lymphangiogenesis by VEGF-C promotes breast cancer metastasis. Nat Med 2001;7:192-8.
[21] Pepper MS, Tille JC, Nisato R, et al. Lymphangiogenesis and tumor metastasis. Cell Tissue Res 2003;314:167-77.
[22] Paavonen K, Puolakkainen P, Jussila L, et al. Vascular endothelial growth factor receptor-3 in lymphangiogenesis in wound healing. Am J Pathol 2000;156:1499-504.
[23] Ji RC, Miura M, Qu P, et al. Expression of VEGFR-3 and 5'-nase in regenerating lymphatic vessels of the cutaneous wound healing. Microsc Res Tech 2004;64:279-86.
[24] Maeda S, Suzuki S, Suzuki T, et al. Analysis of intrapulmonary vessels and epithelial-endothelial interactions in the human developing lung. Lab Invest 2002;82:293-301.
[25] Weibel ER. Stereological methods. Volume 1. Practical methods for biological morphometry. Orlando (Fla): Academic Press; 1979. p. 26-39.
[26] Yamaguchi M, Takahashi T, Togashi H, et al. The corrected collagen content in paraquat lungs. Chest 1986;90:251-7.
[27] Yaegashi H, Takahashi T, Kawasaki M. Microcomputer-aided reconstruction: a system designed for the study of 3-D microstructure in histology and histopathology. J Microsc 1987;146:55-65.
[28] Baluk P, Tammela T, Ator E, et al. Pathogenesis of persistent lymphatic vessel hyperplasia in chronic airway inflammation. J Clin Invest 2005; 115:247-57.
[29] Matsui K, Nagy-Bojarsky K, Laakkonen P, et al. Lymphatic microvessels in the rat remnant kidney model of renal fibrosis: aminopeptidase p and podoplanin are discriminatory markers for endothelial cells of blood and lymphatic vessels. J Am Soc Nephrol 2003;14:1981-9.
[30] Keane MP, Donnelly SC, Belperio JA, et al. Imbalance in the expression of CXC chemokines correlates with bronchoalveolar lavage fluid angiogenic activity and procollagen levels in acute respiratory distress syndrome. J Immunol 2002;169:6515-21.
[31] Ebina M, Shimizukawa M, Shibata N, et al. Heterogeneous increase in CD34-positive alveolar capillaries in idiopathic pulmonary fibrosis. Am J Respir Crit Care Med 2004;169:1203-8.
[32] Renzoni EA, Walsh DA, Salmon M, et al. Interstitial vascularity in fibrosing alveolitis. Am J Respir Crit Care Med 2003;167:438-43.
[33] Cosgrove GP, Brown KK, Schiemann WP, et al. Pigment epithelium-derived factor in idiopathic pulmonary fibrosis: a role in aberrant angiogenesis. Am J Respir Crit Care Med 2004;170: 242-51.
[34] Lappi-Blanco E, Kaarteenaho-Wiik R, Soini Y, et al. Intraluminal fibromyxoid lesions in bronchiolitis obliterans organizing pneumonia are highly capillarized. Hum Pathol 1999;30:1192-6.

Human Pathology (2009) 40, 1278–1287

ELSEVIER

Human
PATHOLOGY

www.elsevier.com/locate/humpath

Original contribution

The definition of fibrogenic processes in fibroblastic foci of idiopathic pulmonary fibrosis based on morphometric quantification of extracellular matrices

Masahiro Yamashita MD[a,*], Kohei Yamauchi MD[b], Ryoji Chiba MD[c], Noriyuki Iwama MD[c], Fumiko Date[a], Naoko Shibata[a], Hiroyuki Kumagai MD[a], Juha Risteli MD[d], Shinobu Sato MD[e], Tohru Takahashi MD[f], Masao Ono MD[a]

[a]*Department of Pathology, Tohoku University Graduate School of Medicine, Sendai, Miyagi 980-8575, Japan*
[b]*Department of Respiratory Medicine, Iwate Medical University, Morioka, Iwate 020-8505, Japan*
[c]*Department of Pathology, Sendai Kosei Hospital, Sendai, Miyagi, Japan*
[d]*Department of Clinical Chemistry, Oulu University, Oulu, Finland*
[e]*Department of Internal Medicine, Saka General Hospital, Shiogama, Miyagi 985-8506, Japan*
[f]*Department of Pathology, Ishinomaki Red Cross Hospital, Ishinomaki, Miyagi 980-8522, Japan*

Received 4 November 2008; revised 27 January 2009; accepted 30 January 2009

Keywords:
Fibroblastic foci;
Extracellular matrix;
Matrix metalloproteinase;
Capillary angiogenesis;
Lymphangiogenesis

Summary There is limited information regarding the process of tissue remodeling in fibroblastic foci associated with idiopathic pulmonary fibrosis. The aim of this study was to identify the different pathologic stages of tissue remodeling in fibroblastic foci based on the histopathologic differences in the glycosaminoglycan distribution and collagen deposition. In addition, we also aimed at clarifying the stage-specific characteristics by taking into consideration the expression pattern of matrix metalloproteinase and angiogenesis. Lung biopsies of 16 patients with idiopathic pulmonary fibrosis were used. The presence of glycosaminoglycans was detected by Alcian blue staining, and type I collagen was detected by immunohistochemical analysis with a primary antibody specific to the cross-linked carboxyterminal telopeptide of type I collagen. The fibroblastic foci characterized by the expression intensity of Alcian blue and telopeptide of type I collagen were divided into 3 groups, namely, Alcian blue^{+}telopeptide of type I collagen^{weak}, Alcian blue^{+}telopeptide of type I collagen^{+}, and Alcian blue^{weak}telopeptide of type I collagen^{+}; consequently, 3 new stages were defined—stages I, II, and III, respectively. A significant inverse correlation was observed between the area densities of Alcian blue^{+} and telopeptide of type I collagen^{+} in fibroblastic foci. Stage I was characterized by the expression of matrix metalloproteinase-2 and tissue inhibitor of matrix metalloprotease-2 in fibroblasts and the overlying epithelium of fibroblastic foci, and also the absence of capillary angiogenesis. In contrast, the expression of these proteins was attenuated in stage III, except for that of matrix metalloproteinase-2 in fibroblasts. In stages II and III, capillary angiogenesis was observed. Lymphangiogenesis was

* Corresponding author.
E-mail address: yamam@mail.tains.tohoku.ac.jp (M. Yamashita).

doi:10.1016/j.humpath.2009.01.014

undetected in all the 3 stages. Thus, pathologic staging helps understand the roles of the factors involved in tissue remodeling in idiopathic pulmonary fibrosis.

1. Introduction

Idiopathic pulmonary fibrosis (IPF) is a chronic and progressive fibrogenic disease of unknown etiology, and it is believed to be a consequence of aberrant healing of a lung injury [1]. IPF is histologically characterized by chronic interstitial pneumonia, small aggregates of myofibroblasts and fibroblasts (termed as fibroblastic foci [FF]), and dense collagen and honeycomb change [2]. FF consist of an extracellular matrix (ECM), overlying epithelium, and a small aggregate of fibroblasts expressing procollagen proteins [2]. It has been considered that FF represent a leading edge of fibrogenesis during the development of IPF [3-7], although the prognostic significance of FF in IPF patients is still controversial [8-10].

A variety of factors that are involved in tissue remodeling of IPF have been examined. The synthesis/degradation of the ECM in FF, in which collagen, cell adhesion protein, and proteoglycans (PGs) are present [11-15], has been of particular interest in this pathologic condition. Matrix metalloproteinase-2 (MMP-2) is a regulator of matrix degradation, and tissue inhibitor of matrix metalloproteinase (TIMP-2) inhibits the activity of MMP-2 by binding to pro-MMP-2. The expression of MMP-2 and TIMP-2 has been observed in fibroblasts and in the overlying epithelium of FF. It has been suggested that these factors play a role in the excessive collagen deposition in the ECM [16-23]. It has also been shown that capillary angiogenesis is involved in tissue remodeling in pulmonary fibrosis [24-29]. In particular, in the case of IPF, $CD34^+$ capillaries are barely detectable in FF [28,29]. It has been speculated that the absence of capillary angiogenesis in FF leads to the poor prognosis of IPF.

There is limited information regarding the fibrogenic processes occurring in FF during the development of IPF. It has been reported that versican—a type of PG that consists of a core protein linked to glycosaminoglycans (GAGs)—is observed in FF and that mature collagen is barely detected in versican-rich lesions [30]. This report suggests that multiple temporal phases may be recognizable in the matrix turnover of FF. In the present study, we performed the pathologic staging of FF by characterizing GAG distribution and collagen deposition in FF. Based on the staging, we investigated the expression patterns of MMP-2 and TIMP-2 and the occurrence of capillary angiogenesis and lymphangiogenesis in FF. In a recent study, lymphangiogenesis has been shown to occur in fibrogenic conditions [31-33]. The pathologic staging of FF provides a deeper understanding of tissue remodeling that occurs during IPF.

2. Materials and methods

2.1. Materials

All lung specimens were obtained by surgical biopsies from 16 patients with IPF, which was diagnosed based on American Thoracic Society/European Respiratory Society criteria [34] and were embedded in paraffin in the Department of Pathology of Iwate Medical University (Morioka, Japan), Ishinomaki Red Cross Hospital (Ishinomaki, Miyagi, Japan), and Saka General Hospital (Shiogama, Miyagi, Japan). Surgical biopsies were required to define the diagnoses of usual interstitial pneumonia. None had any evidence of systemic infection, iatrogenic causes of immunosuppressive agents, toxic exposures, cancer undergoing cytotoxic chemotherapy, preexisting collagen vascular diseases, or cardiac failure. No patient in an accelerated phase of interstitial pneumonia was included. The mean age of patients was 63.3 ± 7.6 (range, 50-78; male:female ratio = 10:6). Normal lung tissues were obtained from 4 patients who died independently of pulmonary diseases. Informed consent was obtained from every patient. The use of all surgical biopsy samples in the present study was approved by the ethical committees of Iwate Medical University, Ishinomaki Red Cross Hospital, and Saka General Hospital.

2.2. Histochemical and immunohistochemical examination

Alcian blue (Al-B) staining was used for the detection of GAGs as previously reported [14,15]. In brief, dewaxed sections were immersed in 100% ethanol for 10 minutes, rinsed in water for 10 minutes, immersed in 3% acetic acid for 2 minutes, and stained in 1% Alcian blue 8GS in 3% acetic acid (pH 2.5) for 1 hour. Nonspecific stain was removed with 3% acetic acid and rinsed in water for 10 minutes. Primary antibodies used in our immunohistochemical analyses are summarized in Table 1. Rabbit polyclonal antibodies to the cross-linked carboxyterminal telopeptide of type I collagen (ICTP) [35] was mainly used as the marker of mature type I collagen. A rat polyclonal antibody to the carboxyterminal propeptide of type I procollagen (PICP) was used for the detection of procollagen protein. The rabbit polyclonal antibody to MMP-2 is known to identify inactive and active forms. CD34 and D2-40 were used as the markers of capillaries and lymphatics, respectively. Deparaffinized tissue sections on glass slides were treated by blocking with 10% normal rabbit or goat serum in phosphate-buffered saline for 15 minutes at room temperature. After rinsing the slides in phosphate-buffered